PHYSICAL REVIEW B **78**, 060503(R) (2008)

Raman-scattering study of $K_xSr_{1-x}Fe_2As_2$ ($x=0.0, 0.4$)

A. P. Litvinchuk,[1,2] V. G. Hadjiev,[1,3] M. N. Iliev,[1,2] Bing Lv,[1,4] A. M. Guloy,[1,4] and C. W. Chu[1,2,5]
[1]*Texas Center for Superconductivity at the University of Houston, Houston, Texas 77204-5002, USA*
[2]*Department of Physics, University of Houston, Houston, Texas 77204, USA*
[3]*Department of Mechanical Engineering, University of Houston, Houston, Texas 77204, USA*
[4]*Department of Chemistry, University of Houston, Houston, Texas 77204, USA*
[5]*Hong Kong University of Science and Technology, Hong Kong, China*
(Received 14 July 2008; published 14 August 2008)

Polarized Raman spectra of nonsuperconducting $SrFe_2As_2$ and superconducting $K_{0.4}Sr_{0.6}Fe_2As_2$ (T_c =37 K) microcrystals are reported. All four-phonon modes ($A_{1g}+B_{1g}+2E_g$) allowed by symmetry are found and identified. Shell model gives reasonable description of the spectra. No detectable anomalies are observed near the tetragonal-to-orthorhombic transition in $SrFe_2As_2$ or the superconducting transition in $K_{0.4}Sr_{0.6}Fe_2As_2$.

DOI: 10.1103/PhysRevB.78.060503 PACS number(s): 74.70.−b, 74.25.Kc, 63.20.D−, 78.30.−j

The renewed interest in superconductors was sparked recently by the discovery of a class of iron-arsenide-based oxypnictides RFeAs$O_{1-x}F_x$ (where R is a rare-earth element).[1–5] Similarly to the cuprate superconductors, doping of superconducting FeAs planes in oxypnictides determines one of the key characteristics of a given material (its superconducting transition temperature), which reaches values as high as T_c=54 K. Oxypnictides were shown to exhibit n-type conductivity. More recently a series of compounds with similarly structured FeAs planes, but with different charge reservoir block $A_xM_{1-x}Fe_2As_2$ (where A is an alkali element and M is Sr or Ba), was found to exhibit superconducting properties.[6] Unlike oxypnictides these superconductors clearly show p-type conductivity.[7] Optimal material doping is achieved in this latter system at $x\approx 0.4-0.5$ when the critical temperature reaches $T_c\sim 38$ K.[8]

First-principles electronic band-structure calculations of oxypnictides point toward unconventional superconductivity that is mediated by antiferromagnetic spin fluctuations.[9–11] Due to rather weak electron-phonon interactions, it is generally believed that the phonons do not contribute substantially to the superconductivity. Despite this fact, it is important to experimentally identify the symmetry and frequency of phonon excitations and search for specific features in the Raman-scattering spectra, which could shed light onto the properties of the superconducting state. In this Rapid Communication we report the results of polarized Raman-scattering studies of $K_xSr_{1-x}Fe_2As_2$ microcrystals for the parent $x=0$ compound and superconducting material with x =0.4. We also present the results of shell-model lattice dynamics calculations, which are in a good agreement with the experimental data.

The compounds under investigation were prepared by high-temperature solid-state reactions of high-purity K and Sr with FeAs as described elsewhere.[8] For the mixed-metal samples $K_xSr_{1-x}Fe_2As_2$, stoichiometric amounts of the ternary iron arsenides were thoroughly mixed, pressed, and then annealed within welded Nb containers (jacketed in quartz) at about 900 °C for 70–120 h. The bulk samples containing microcrystals of typical size of $50\times 50\times 2$ μm^3 were characterized by x-ray diffraction, resistivity, magnetic-susceptibility, Hall, and thermoelectric power measurements.[8,12]

Raman-scattering measurements were performed with a triple Horiba JY T64000 spectrometer equipped with an optical microscope, microcryostat, and liquid-nitrogen-cooled CCD detector. At room temperature a ×100 objective was used to both focus the laser beam (λ_{las}=638.2 nm) at a spot 1–2 μm in diameter on selected ab or ac/bc microcrystal surfaces oriented in an exact scattering configuration and collect the scattered light. For low-temperature measurements the sample was mounted in an optical Microstat^{He} (Oxford Instruments) and long-focus objective (×50 and spot size 2–4 μm, still much smaller than the microcrystal dimensions) was used. The spectra in this case were obtained from crystal surfaces with such orientation that the two strongest phonon modes could simultaneously be observed. The excitation power density did not exceed 10^4 W/cm^2 in order to minimize heating of the sample. Similarly to the case of RAsFeO (Ref. 13), the Raman intensities were very low and long acquisition times were needed.

AFe_2As_2 crystallizes in the tetragonal $ThCr_2Si_2$-type structure with space group $I4/mmm$ (D_{4h}^{17}).[14] The unit cell parameters and atomic positions were obtained from powder-diffraction data using Rietveld refinement. The atomic positions were consistent with the literature values. The cell parameters for $SrFe_2As_2$ are a=0.39259(2) nm and c =1.2375(1) nm. For $K_{0.40}Sr_{0.60}Fe_2As_2$, a=0.38898(2) nm and c=1.2948(1) nm; z_{As}=0.3516 for both compounds. The structure features individual FeAs layers identical to those in RFeAsO but with a different layer stacking sequence (AA in RFeAsO and AB in the $ThCr_2Si_2$-type structure).

From symmetry considerations[15] one expects four Raman-active phonons: A_{1g}(As), B_{1g}(Fe), E_g(As), and E_g(Fe) (Table I). Using the polarization selection rules and the fact that the ab surfaces could easily be visually recognized, the identification of the Raman line symmetry is straightforward. In particular, in the spectra obtained from the ab plane, the intensity of the A_{1g} mode will remain constant for any orientation of the incident polarization $\vec{e}_i$ given that the scattered polarization $\vec{e}_s$ is parallel to it ($\vec{e}_s \| \vec{e}_i$) and will be zero in any crossed polarization configuration ($\vec{e}_s \perp \vec{e}_i$). The intensity of the B_{1g} mode, however, depends on the angle α between $\vec{e}_i$ and the a axis being proportional to $\cos^2 2\alpha$ for parallel and $\sin^2 2\alpha$ for crossed configuration.

TABLE I. Wyckoff positions and irreducible representations for $SrFe_2As_2$ (space group $I4/mmm$, No.139), which yield Brillouin-zone-center modes. Lower part of the table lists experimental and calculated mode frequencies and their activity.

Atom	Wyckoff position	Γ-point phonon modes
Sr	$2a$	$A_{2u}+E_u$
Fe	$4d$	$A_{2u}+B_{1g}+E_g+E_u$
As	$4e$	$A_{1g}+A_{2u}+E_g+E_u$

Modes classification

$$\Gamma_{\text{Raman}}=A_{1g}+B_{1g}+2E_g$$

$$\Gamma_{\text{IR}}=2A_{2u}+2E_u$$

$$\Gamma_{\text{Acoustic}}=A_{2u}+E_u$$

Raman tensors

$$A_{1g}(x^2+y^2,z^2)\rightarrow\begin{bmatrix}a&0&0\\0&a&0\\0&0&b\end{bmatrix}$$

$$B_{1g}(x^2-y^2)\rightarrow\begin{bmatrix}c&0&0\\0&-c&0\\0&0&0\end{bmatrix}$$

$$E_{g_1}(xz),E_{g_2}(yz)\rightarrow\begin{bmatrix}0&0&-e\\0&0&0\\-e&0&0\end{bmatrix},\begin{bmatrix}0&0&0\\0&0&e\\0&e&0\end{bmatrix}$$

Mode	Type	Expt. cm^{-1}	LDC cm^{-1}	Main atomic displacements	Allowed polarizations
A_{1g}	Raman	182	183	As(z)	XX, YY, ZZ
B_{1g}	Raman	204	203	Fe(z)	XX, YY, $X'Y'$
E_g	Raman	114	111	As(xy), Fe(xy)	XZ, YZ
E_g	Raman	264	335	Fe(xy), As(xy)	XZ, YZ
A_{2u}	IR		198	Sr(z), As($-z$)	Z
A_{2u}	IR		322	Fe(z), Sr($-z$)	Z
E_u	IR		135	Sr(xy)	X, Y
E_u	IR		263	Fe(xy), As($-xy$)	X, Y

Figure 1 shows the variations with α of the Raman spectra of $SrFe_2As_2$ obtained from the ab plane. Only one line at 204 cm^{-1} is clearly pronounced in the spectra and its intensity follows the angular dependence expected for the B_{1g} mode. Obviously, the intensity of the A_{1g} mode is negligible for incident light propagating along the c axis and polarized in the ab plane. However, all Raman-active phonons are clearly seen in the spectra taken from $ac(bc)$ surface as illustrated in Fig. 2. These observations suggest the following relations between the elements of the Raman tensor in Table I: $|b|\gg|a|$ and $|c|\gg|a|$. The experimental phonon frequencies are listed in Table I.

We also performed shell-model calculations of the lattice dynamics using the general utility lattice program (GULP),[16] which is known to reasonably describe a wide class of ionic materials (oxides in particular).[17,18] In the shell model each ion is considered as a point core with charge Y surrounded by a massless shell with charge Q. The free-ion polarizability is accounted for by the force constant k. The short-range potentials $V(r)$ are chosen in the Born-Mayer-Buckingham form

$$V(r)=a\exp(-r/r_0)-cr^{-6}.$$

The model parameters of Fe^{2+}, Sr^{2+}, and As^{3-} were tuned in order to achieve the best agreement with experimental even-parity phonon modes (to the best of our knowledge, there is no experimental information on odd-parity infrared-active phonons); they are listed in Table II. The displacement patterns of all four Raman-active modes are shown in Fig. 3. It is worth noting here that, while the A_{1g} and B_{1g} modes can be considered as "pure" modes (involving displacements

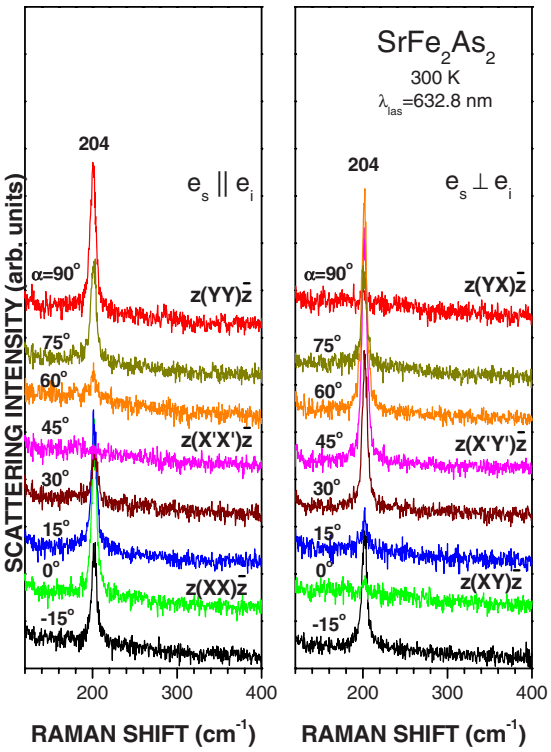

FIG. 1. (Color online) Raman spectra of $SrFe_2As_2$ for a series of *ab*-plane-polarized scattering geometries. Numbers on the left denote the angle α between incident light polarization and the crystallographic *a* axis.

along the *c* axis of either As or Fe), the two E_g modes are strongly mixed. As expected, the A_{1g} and B_{1g} modes of $SrFe_2As_2$ are very close in frequency to the corresponding modes of same symmetry in *R*FeAsO.[13] Indeed, the individual FeAs layers in both compounds are practically identical in terms of bond lengths and angles.

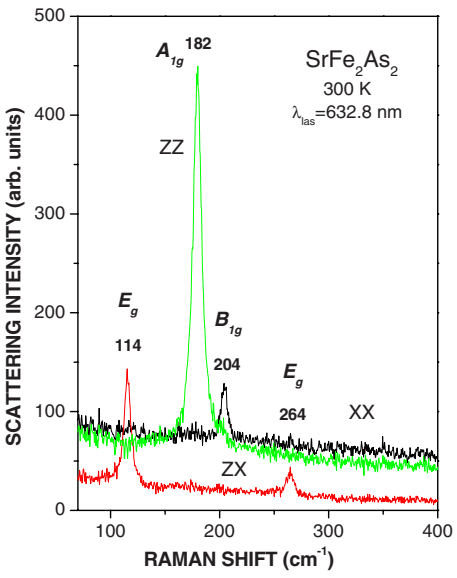

FIG. 2. (Color online) *XX* ($A_{1g}+B_{1g}$ modes allowed), *ZX* (E_g), and *ZZ* (A_{1g}) spectra of $SrFe_2As_2$ as obtained from *ac* surface at room temperature.

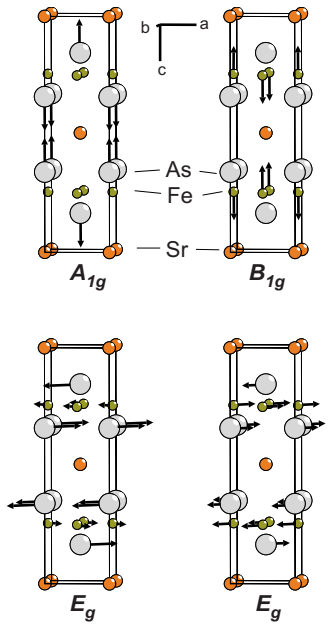

FIG. 3. (Color online) Displacement patterns of Raman-active modes of $SrFe_2As_2$ from the shell-model calculations.

Due to the long acquisition time, the Raman spectra of superconducting $K_{0.4}Sr_{0.6}Fe_2As_2$ (T_c=37 K) microcrystals were taken from the surface where both A_{1g} and B_{1g} modes were observed (Fig. 4). Their frequency is practically the same as in the parent compound, the linewidth being somewhat larger. Upon lowering temperature these two modes show standard anharmonic behavior in both materials with

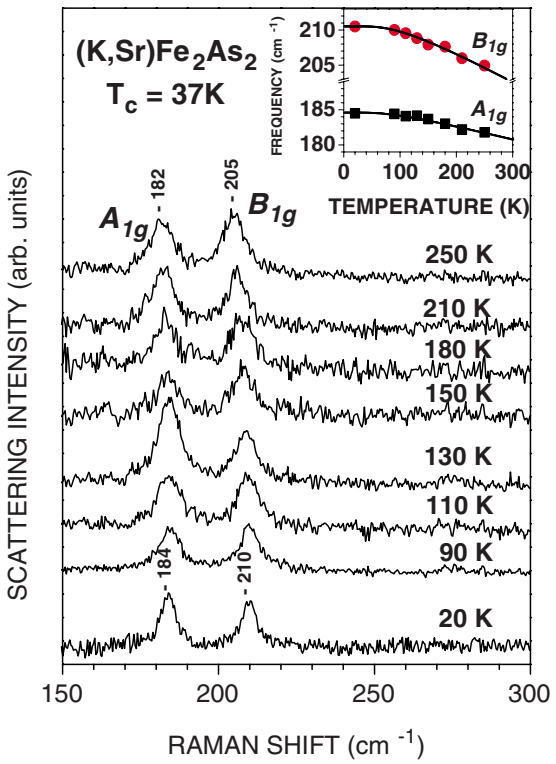

FIG. 4. (Color online) Temperature-dependent Raman spectra of $K_{0.4}Sr_{0.6}Fe_2As_2$.

TABLE II. Shell-model parameters and the short-range potentials for $SrFe_2As_2$. We used structural parameters reported in Ref. 8 and listed in the text.

Ion	$Y(\|e\|)$	$Q(\|e\|)$	$k(\text{eV}\times\text{Å}^{-2})$	Ion pair	a (eV)	r_0(Å)	$c(\text{eV}\times\text{Å}^6)$
Sr	2.40	−0.50	10.0	Sr-As	1226	0.482	0
Fe	2.40	−0.50	19.9	Fe-As	2399	0.350	0
As	0.15	−3.00	15.2	As-As	2000	0.209	2500

rather moderate frequency and width variations as illustrated in Fig. 4 for $K_{0.4}Sr_{0.6}Fe_2As_2$. No phonon anomalies either near the tetragonal-to-orthorhombic structural transition of $SrFe_2As_2$ at $T_{t-o}\approx 203$ K (Ref. 19) or below $T_c=37$ K of $K_{0.4}Sr_{0.6}Fe_2As_2$ were observed within the accuracy of our experiments for the A_{1g} and B_{1g} modes. In principle, the main effect of the structural transition should be a splitting of the E_g modes, which position was difficult to follow in the temperature-dependent experiments. The reported anisotropy of Fe-As bond lengths within *ab* plane, however, is only 0.55%.[19] Following a simple expression[13] for the phonon frequency ω_{ph} as a function of bond length l ($\omega_{\text{ph}}^2\sim 1/l^3$), one might expect splitting of the modes by about 0.8%. Even for the high-frequency E_g mode at 264 cm^{-1} this yields 2.1 cm^{-1}, which is small compared to the linewidth and is challenging to be observed experimentally.

In conclusion, all four Raman-active phonons in $SrFe_2As_2$ have been observed experimentally. The substitution of K for Sr has little effect on the frequencies of Raman modes involving As and Fe vibrations. The structural transition in $SrFe_2As_2$ and superconducting transition in $K_{0.4}Sr_{0.6}Fe_2As_2$ do not produce detectable anomalies in the parameters of A_{1g} and B_{1g} modes.

This work was supported in part by the T.L.L. Temple Foundation, the J.J. and R. Moores Endowment, the State of Texas through TCSUH, the USAF Office of Scientific Research, and the LBNL through US DOE. B.L. and A.M.G. acknowledge the support from the NSF (Grant No. CHE-0616805) and the R.A. Welch Foundation. We are grateful to Zhongjia Tang for the help with crystallographic calculations.

[1] Y. Kamihara, T. Watanabe, M. Hirano, and H. Hosono, J. Am. Chem. Soc. **130**, 3296 (2008).
[2] H. Takahashi, K. Igawa, K. Arii, Y. Kamihara, M. Hirano, and H. Hosono, Nature (London) **453**, 376 (2008).
[3] X. H. Chen, T. Wu, G. Wu, R. H. Liu, H. Chen, and D. F. Fang, Nature (London) **453**, 761 (2008).
[4] P. M. Grant, Nature (London) **453**, 1000 (2008).
[5] T. Y. Chen, Z. Tesanovic, R. H. Liu, X. H. Chen, and C. L. Chien, Nature (London) **453**, 1224 (2008).
[6] M. Rotter, M. Tegel, and D. Johrendt, arXiv:0805.4630 (unpublished).
[7] G. F. Chen, Z. Li, G. Li, W. Z. Hu, J. Dong, X. D. Zhang, P. Zheng, N. L. Wang, and J. L. Luo, Chin. Phys. Lett. **25**, 3403 (2008).
[8] K. Sasmal, B. Lv, B. Lorenz, A. Guloy, F. Chen, Y. Xue, and C. W. Chu, arXiv:0806.1301 (unpublished).
[9] D. J. Singh and M. H. Du, Phys. Rev. Lett. **100**, 237003 (2008).
[10] L. Boeri, O. V. Dolgov, and A. A. Golubov, Phys. Rev. Lett. **101**, 026403 (2008).
[11] I. I. Mazin, D. J. Singh, M. D. Johannes, and M. H. Du, Phys. Rev. Lett. **101**, 057003 (2008).
[12] B. Lorenz, B. Lv, and A. M. Guloy (unpublished).
[13] V. G. Hadjiev, M. N. Iliev, K. Sasmal, Y.-Y. Sun, and C. W. Chu, Phys. Rev. B **77**, 220505(R) (2008).
[14] S. Rozsa, and H. U. Schuster, Z. Naturforsch. B **36**, 1668 (1981).
[15] D. L. Rousseau, R. P. Bauman, and S. P. S. Porto, J. Raman Spectrosc. **10**, 253 (1981).
[16] G. D. Gale, J. Chem. Soc., Faraday Trans. **93**, 629 (1997).
[17] V. N. Popov, J. Phys.: Condens. Matter **7**, 1625 (1995).
[18] M. N. Iliev, M. V. Abrashev, A. P. Litvinchuk, V. G. Hadjiev, H. Guo, and A. Gupta, Phys. Rev. B **75**, 104118 (2007).
[19] M. Tegel, M. Rotter, V. Weiss, F. M. Schappacher, R. Pöttgen, and D. Johrendt, arXiv:0806.4782 (unpublished).